Application of the 3D-DGI Method for Selection of the "Best" ADC & Amplifier Combination From the Measured Trendless Sequences

RR Nigmatullin[1*], RK Sagdiev[1]

Department of Material Sciences & Engineering, Kazan National Research Technical University, Tatarstan, Russian Federation

Abstract

3D-DGI (Discrete Geometrical Invariants) method allows to reduce initial rectangle matrices N×M (N-is number of data points, M < N is number of columns) to a matrix M× P (P=13), where P – represents a set of invariants combined from of the first, second, third and the fourth moments inclusive. This "universal" platform allows to compare any random trendless sequences (TLS) with each other. The further analysis shows that one can extract only two significant parameters/criteria (free from treatment and model errors) for comparison of TLS recorded from the given set of ADCs. The experimental data set represented 15 rectangle matrices with parameters N=20000, M=150 (filtered in the region 1.1-5.0 kHz) and 15 matrices that were not subjected to the filtration procedure. The proposed algorithm given in the paper allows to select the "best" ADC&Amplifier combination from the given ones based on analysis of their TLS(s) and proposed criteria. The authors think that the algorithm can find a wide application in the industrial electronics based on the simplicity, reproducibility and reliability of the proposed procedure.

Key words: 3D-DGI method • Trendless sequences • Proposed criteria for selection of the "best" ADC&Amplifier combination

Introduction

The hidden information that is contained in different TLs(s) and their extraction with the help of new method. 3D-Discrete Geometrical Invariants (DGI) method; ADC noises and its hidden information; Reduction of rectangle matrices to small amount of quantitative parameters [1].

Noise diagnostics equipment in recent years is widely used to monitor the quality and reliability of equipment. This method combines the small-time expenses and no risk of damage to the component in question [2].

It is known three main methods used in noise diagnostics. These include the Fourier transform of the noise signal, wavelet analysis, and flicker noise spectroscopy. A brief description and comparison of these methods are given in table 1. Other methods with their merits and demerits proposed by the professors Timashev S.F. and Yulmetyev R.M. are discussed in paper [3].

The existing method	Conditions of its application and merits	Possible limitations and the limits of its applicability	Comments
Fourier transformation	The calculation and subsequent analysis of the frequency spectrum of a signal using Fourier transform. Good elaboration of the theory of spectral analysis of signals.	It is applicable when signals are stationary. Difficulty of analysis in terms of changes of the calculated spectrum in time. Limited accuracy at low frequencies. The Gibbs "oscillation" phenomenon related to the transformation of rectangle signals contains large unremovable error.	Some set of the calculated frequencies does not belong to the system considered. The F-transform is used independently and not as a fitting function for description of a signal S(t).
Wavelet transform	Decomposition of a signal into functions of finite duration (wavelets). The method is especially effective when at the slow signal component background, a	Insufficient elaboration of the theory of analysis. Lack of criteria for choosing the basis of signal decomposition.	Contains uncontrollable errors especially related to application of the specific types of wavelets to the chosen random sequence. Each type of wavelet, being applied to

	relatively fast component may appear		the same TLS, contains the specific error.
Flicker noise spectroscopy	According to this theory, electrical noise is the result of an irreversible evolution of a multilevel hierarchical system from a variety of noise sources. Each level has its own space-time organization.	It is difficult to separate this type of noise from the mixture of others, including heat, the Schottky's and other type of noises. The physical nature of this noise, in spite of its wide propagation, is still remained as unknown.	The frequency behavior of the flicker-noise is definitely known at low frequencies -) (S, while for the wide frequency range it is a subject of discussion.

Table 1: Comparison of the basic noise analysis methods.

The described methods make it possible to carry out flaw detection of components and entire blocks of equipment. This task can also be extended to the case of choosing the best component or block among the existing ones.

The question arises, is it possible to propose a simple method, which enables to select the "best" component or block (ADC&Amplifier combination in our case) from the existing ones? The method should be rather general and simple, having the minimal computation cost and algorithmically simple being embedded into some microcontroller device.

In this paper, based on the 3D-DGI method we want to propose a simple algorithm that enables to select the "best" ADC&Amplifier combination among the existing ones. The proposed procedure one can find a wide application in the industrial electronics, where it is necessary to test/sort some devices based on their TLS.

Experimental Part

A non-inverting amplification cascade on an operational amplifier is used as a noise/random fluctuation source. The used electrical circuit is shown in Fig.1. R3 is the signal source equivalent impedance for the amplifier. The gain of the first stage is set by the ratio of resistors R1/R2. Since the noise amplitude considered as the output of the first stage is small and does not exceed the ADC noise, the second stage of the amplifier on U2 is used. As a result, the ADC noise is not noticeable against the background of the connected amplifier noise. The second stage of the amplifier also does not contribute significantly to the overall noise. The first stage has a gain of 101, the second stage has a gain of 200.

The LM224 quad operational amplifier were used in these amplification cascades. Since there are four operational amplifiers embedded into the LM224 chip, it is possible to build two amplifiers as it is shown in Fig. 1 for one chosen chip. We examined 15 LM224 chips and 30 amplifiers, respectively. An amplifier circuit board was made containing a socket, where the LM224 chip was embedded. Thus, a possible "identity" of the amplifier circuits was ensured.

We should notice that LM224 is a very cheap operational amplifier and no conventional noise parameters are given in its datasheet specification. Even the word "noise" cannot be found in their covering documents.

Elvis II workbench by National Instruments was used as ADC. Elvis II has 1.25 MS/s (Mega samples per second) maximum sampling rate and 16-bit resolution.

The sampling frequency in the experiment was set to 10 kHz. To prevent external interference, the measured TLS was digitally filtered with a bandwidth between 1.1 kHz and 5 kHz.

For each amplifier, 135 measurements were successively carried. Each measurement contains 20000 data points. Therefore, one set of measurements represents itself a rectangle matrix M(with N=20000 - data points, M=135 includes all successive measurements/columns). After digital filtering, the initial portion of the measured signal containing a possible transient regime was cutoff. In the measurement procedure, amplifier noise is added to the measured signal.

Description of the Algorithm

For solution of the main problem one can apply the 3D-DGI (Discrete Geometrical Invariants) -method. Partly it was described in paper [8]. In this work we choose the complete version. It is described in the Mathematical Appendix. As it follows from expression (A14a), this method gives a "universal" platform, which allows to compress an initial matrix M(N×M) Yj(m) (j=1,2,..,N is a number of data points/ matrix rows, m=1,2,...,M (M < N) is a number of columns/successive measurements) to the matrix Mc(M×P) ym(p)(p=1,2,…P). This reduced matrix has P=13 columns only, which are distributed as follows: (p=1-3: <yα> - gravity centers or correlations of the first order; p=4-6 for R(α,β)(3) -the reduced correlations of the third order; p=7-12, α,β = 1,2,3 for Aαβ(6) -correlations of the second order; P=13 I4(1) -the reduced correlation of the fourth order.). They determine the complete combination of the moments and their intercorrelations (3+3 +6+1=13) up to the fourth order inclusive. In the result of application of the 3D-DGI method we obtain (P=13) distributions ym(p) that demonstrate the variations of each statistical parameter with respect to the number of columns/repeated measurements (m=1,2…,M).

The further reduction is possible if one takes into account that each random function ym(p) for the fixed value of p is located inside the rectangle Range(m) (Range[ym(p)]), where Range(f)=max(f) – min(f). For comparison of one random function y1,m(p) with another y2,m(p) corresponding to the fixed column p one can use the following simple formula.

$$Q_{1,2}(p) = \frac{Range(y_{1,m}(p)) + Range(y_{2,m}(p))}{\max(y_{1,m}(p), y_{2,m}(p)) - \min(y_{1,m}(p), y_{2,m}(p))}, \qquad (1)$$

This expression in spite of its simplicity is really effective for comparison of the statistical closeness of a pair random functions belonging to the given/another sampling participating in comparison operation of two matrices having the statistically close columns. Really, if the function Q1,2(p) is located in the interval [1,2] then the pair random functions are statistically close to each other. In the case when Q1,2(p) (0,1) one can conclude that the pair random functions compared from two matrices y1,m(p) and y1,m(p) are statistically different. Besides this important parameter given by expression (1), one can take into account the symmetry of the random function ym(p). Any random function located in the rectangle)m(egnaR(Range[y(m)]) crosses the line <ym(p)> coinciding with its

mean value. Therefore, for evaluation of the symmetry of a random function one can introduce the value

$$Sm(y(p)) = \frac{mean(y_m(p)) - 0.5 \cdot \left(\max(y_m(p)) + \min(y_m(p))\right)}{Range(y_m(p))}, \quad (2)$$

for any fixed p. If the value Sm(y) is located near zero (Sm(y))0 then the line mean(y) <y> divides the rectangle)m(egnaR(Range[y(m)]) on two almost equal parts. In other cases, the value Sm(y) located in the interval [-1/2, 1/2)] determines the measure of asymmetry. After application of expression (1) for comparing of similar columns (belonging to the fixed p) one can receive finally the vector V(p) of the length P=13 that contains information about the statistical closeness of two compared matrices. This vector can be used for comparison of the "pattern" initial matrix with the rest tested ones. What we should do in cases, when the "pattern"/"best" matrix is absent? Therefore, the problem is formulated as follows: how to choose the "best" matrix from the given ones based on simple criteria that are free from treatment errors and model assumptions? In this case, one can suggest two simple criteria based on the following observations. Let us normalize the compressed matrix ym(p).

$$yn_m(p) = \frac{y_m(p) - \langle y_m(p) \rangle}{Range(y_m(p))}, \quad Range(yn_m(p)) = 1, \quad (3)$$

In order to receive the value of the range of the normalized function (3) equals one for any value of p. After integration of (3) with respect to its mean value we obtain the matrix Jym(p). If one calculates the range of the integrated matrix Range(Jym(p)) with respect to all equivalent columns p then we receive the vector J(p). If one evaluates the Range(J(p)) we obtain finally only one parameter that can be used for comparison of the chosen rectangle matrix with another one. Another important parameter is associated with calculation of the asymmetric parameter Sm(J(p)) in accordance with expression (2) for all values of p. Schematically, the final stage allowing to select two parameters from the initial rectangle matrices among the given ones can be expressed as

$$\mathbf{M}(N \times M) \rightarrow \mathbf{Mc}(M \times P) \rightarrow J(p) \rightarrow \left[Range(J(p))\right] \rightarrow \min\left[Range(J(p))\right],$$
$$\mathbf{M}(N \times M) \rightarrow \mathbf{Mc}(M \times P) \rightarrow J(p) \rightarrow \left[Sm(J(p))\right] \rightarrow \min\left[\left|Sm(J(p))\right|\right]. \quad (4)$$

On the right-hand side, we have only two parameters that can be associated with selection of the "best" parameters and serve as simple criteria based on their minimal values. In addition to S/N criterion these two parameters are associated with stability and robustness of the measured TLS expressed in the form of rectangle matrices. Here we should stress again that these two criteria are free from treatment errors and the model errors including a priory-imposed probability assumption.

It is interesting to notice that simple expression (1) can be used also for comparison each successive measurement with another one presented in the given rectangle matrix [N M]. If one compares the vectors ym forming the columns of the initial matrix with each other, then, in the result of application (1), one can obtain the symmetrical matrix U(m1,m2) (m1,2 =1,2,...,M) with elements located in the interval 0 ≤ U(m1,m2) ≤ 2. Only elements located in the interval 1 ≤ U(m1,m2) ≤ 2 will correspond to a "good" experiment; while the elements from the interval 0 ≤ U(m1,m2) < 1 should be considered as possible "outliers" and correspond to a "bad"/unsuccessful

experiment. In the same manner, one can compare with the help of (1) two different matrices U(j,m) and V(j,m) having the same number of columns.

Data Treatment Procedure

In the result of experiments described in section 2 we receive 60 rectangle matrices. Each matrix contains N=20000 data points and M=135 columns. The first 30 ADC connected with amplifiers were filtered in the range (1.1-5.0 kHz) in order to suppress possible interferences that would disturb the recorded TLS(s). Each tested amplifier was connected with the ADC and the pair connected amplifiers (as it is shown in Fig.1) were considered as "identical" to each other, however, their influence on the recorded signal can be slightly different. Other 30 matrices were recorded in the same conditions, however, there TLS(s) were not filtered. We repeat the problem that we are going to solve because of its importance: Is it possible to choose the "best" ADC&Amplifier combination based on two simple statistical criteria proposed in section three? The proposed algorithm can be divided on three basic steps.
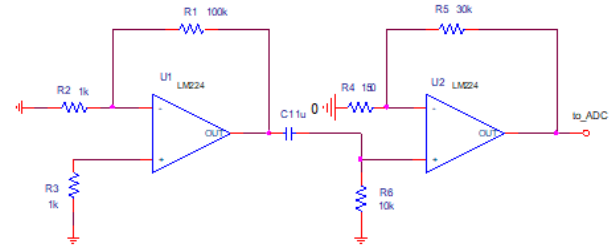
Figure 1: The experimental setup of the electric circuit, used in the experimental measurements. All explanations are given in the text.

Step 1. Reduction to three incident points.

In order to decrease the computational cost related to treatment of the large-size rectangle matrices, we use the procedure of reduction to three incident points. This procedure was described earlier in papers [9-11]. The essence of this procedure is the following: we choose initially b (3 < b << N) points and select from them only three incident/important points (max(b), mean(b) and min(b)) that are remained invariant relatively [b]! permutations. If one can form three compressed distributions Yupj(m), Ymnj(m) and Ydnj(m) corresponding to maximal, mean and minimal values, accordingly, and take their averaged value Yavj(m) = (1/3)Y(upj(m)+Ymnj(m)+Ydnj(m)), then we obtain the compact/compressed set of TLS(s) that it is suitable for the further analysis. For a certain value of the compressed parameter b it is possible to prove that the compressed data Yavj(m) is similar to initial data Yj(m). In order to compare their similarity, one can use the statistics of the fractional moments. This generalized statistic allows to compare TLS(s) having different samplings. In our case, at b=10 the value of the Pearson correlation coefficient applied for comparison of the generalized mean values (see the definition in [5]) formed from the TLS Yavj(m) and Yj(m) is located in the interval [0.95-0.99]. Therefore, one concludes that compression in ten times (b=10) keeps the similarity between the initial sequences Yj(m) and their compressed replicas Yavj(m) and considerably facilitate their further calculations. These two compared sequences are shown in Fig.2. In a similar manner, we prepared 60 compressed matrices using the same value b=10.
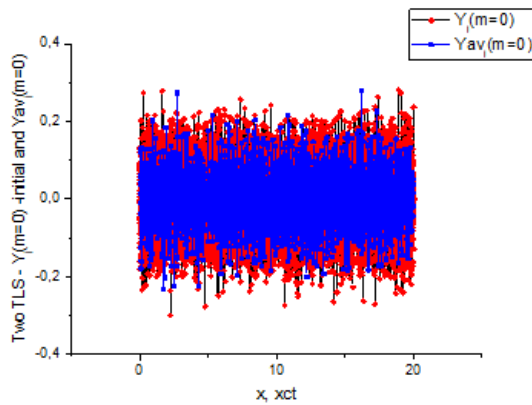
Figure 2: The comparison of initial noise (red points) with the compressed noises realized with the help of reduction to three incident points procedure (b=10). They are similar to each other. The Pearson correlation coefficient lies in the interval [0.95-0.99]. For comparison, we demonstrate the filtered data of the rectangle matrix corresponding to combination ADC&Amplifier "1". The same procedure was realized for all available 60 matrices.

It is interesting also to compare the quality of the performed experiment with the help of expression (1). The comparison of the compressed data (calculated with the help of expression (1)) for the rectangle matrix corresponding ADC&Amplifier-1.1 combination for the filtered data is shown in Fig.3. As it follows from this figure all correlations are concentrated in the interval [1.604-1.998] and "bad" measurements (less than one) are absent. All other 59 matrices are tested in the same manner and possible outliers and "bad" measurements were not found.
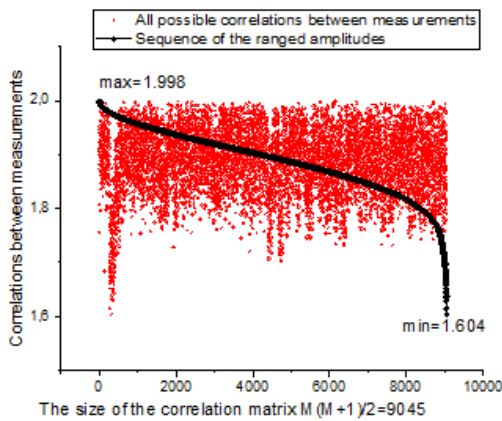
Figure 3: The correlation between successive measurements calculated with the help of expression (1) for the same rectangle matrix corresponding to combination ADC&Amplifier "1". The interval of correlations is clearly shown also. The black solid line shows the sequence of the ranged amplitudes.

Step 2. The usage of 3D-DGI method.

As it has been explained in the previous chapter and in the Mathematical Appendix, this method "prepares" a "universal" platform for compression of an initial rectangle matrix M(N×M) Yj(m) to the matrix Mc(M×P) ym(p) (p=1,2,…P) having P=13 columns, composed from the moments and their intercorrelations up to the

fourth order inclusive. In our case, we compressed all 60 matrices and received the set of the compressed matrices for their further comparison. A typical surface for the first column of the rectangle matrix corresponding the previous ADC&Amplifier-1.1 combination for the filtered data is shown in Fig.4.
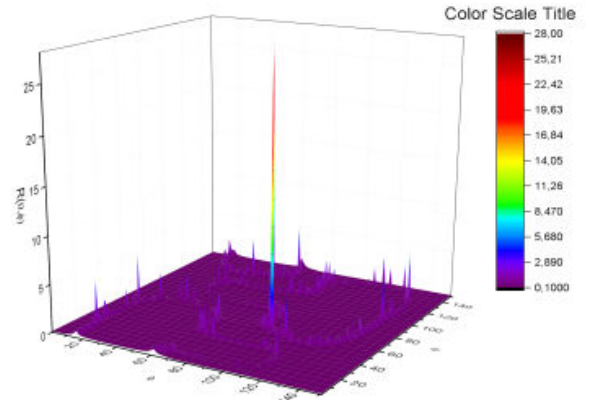
Figure 4: Typical surface calculated for the compressed curve ym=0(p). These peaks demonstrate the sensitivity of different moments to variations of the matrix Mc(M.snmuloc)P

Step 3. The final comparison of all filtered/nonfiltered data.

The final comparison is realized with the help of the scheme (4). We skip some intermediate parameters and demonstrate only Range[J(p)] and Sm[(J(p)] for each compared matrix. The key figures 5(a,b) and 6(a,b) show clearly how to select the "best" combination [ADC&Amplifier-n, (n+0.5), where the integer numbers n=1,2,…,15 numerate the first amplifier, while the half-integer numbers n=1.5, 2.5,…,15.5 belong to the combination of ADC with the second amplifier. As it follows from simple analysis the best selection belongs to combination "4", the second place corresponds to the combination "14.5" the "worst" combination is "6.5".
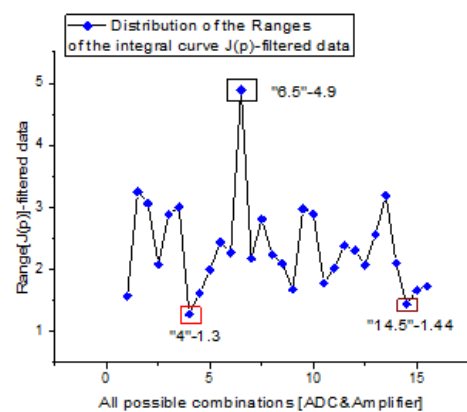
Figure 5(a): This key figure demonstrates the distribution of the Range[J(p)] covered all possible combinations of ADC with types of amplifiers -one type is marked by integer numbers: 1,2,…,15, while the second type is marked by semi-half values 1.5,2.5, …,15.5. As it follows from this simple analysis the best selection belongs to combination "4", the second place occupies the combination "14.5" the "worst" combination is "6.5".
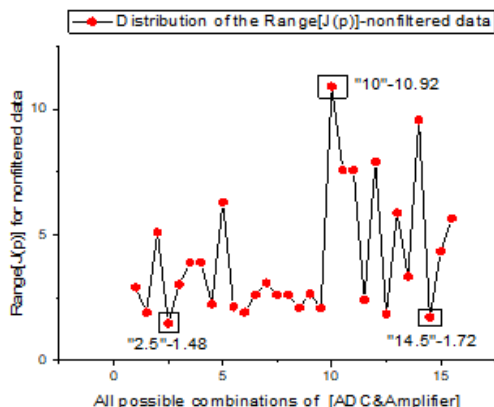
Figure 5(b): This figure demonstrates the influence of the filtration procedure. The ranges are increased and combinations are changed. It means that filtration procedure is important.

The distribution of symmetry parameter Sm[J(p)], which should accept also the minimal values and shown in Fig.6(a) confirms the selection of the combination "4" and "14.0", occupying the second place. The "worst" place is changed.
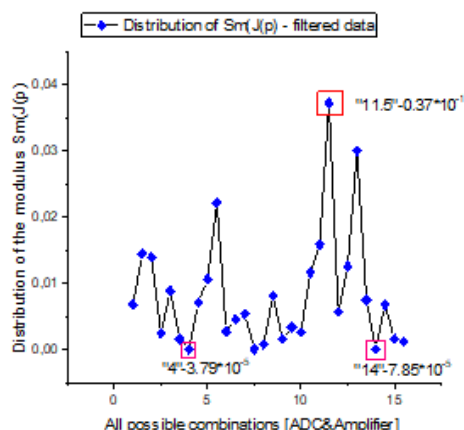
Figure 6(a): The distribution of symmetry parameter Sm[J(p)], which should accept also the minimal values confirms the selection of the combination "4" and "14.0", occupying the second place. The "worst" place is changed. This conclusion is valid for the filtered data

This conclusion is valid for the filtered data. The figures 5(b) and 6(b) prove that filtration procedure is important. They select other combinations as "2.5" and "14.5" and in in Fig. 6(b) there is a whole region with the values located in the interval [7.37 10-4, 1.31.]3-01 One can notice also that their minimal values are higher with comparison with values subjected to the filtration procedure.
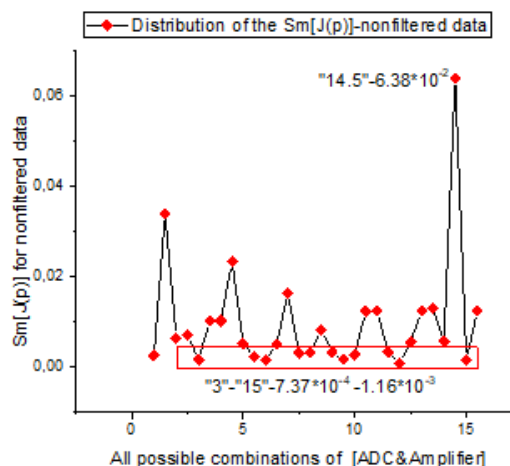
Figure 6(b): For nonfiltered data the distribution of Sm[J(p)] is different. We have combinations "3"-"15" [ADC&Amplifiers] located in the vicinity of zero value, however these combinations are not sufficient for the selection of the "best" one. Comparison the data of this figure with Fig. 5(a) allows to notice that the values Sm[J(p)] for the filtrated data is smaller and are closer to zero value.

Figure 7 demonstrates the distribution of minimal values (realized with the help of expression (1)) and shows clearly the result of the filtration procedure. All filtered data become more correlated with each other, while uncorrelated data giving the values less than one can be considered as "dirty" data subjected by the influence of some uncontrolled external factors.
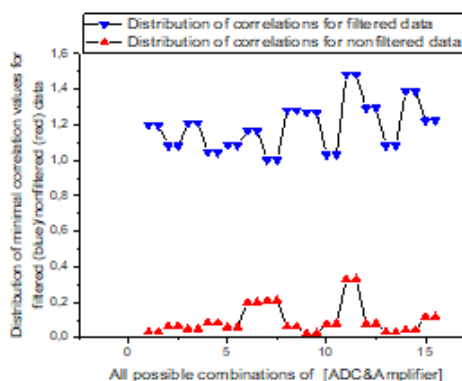
Figure 7: This figure demonstrates clearly the significance of the filtration procedure. If we compare the minimal values realized for the both cases then one can notice that the filtered data are more compact and closer to each other (the values of the correlation parameter are higher) in comparison with unfiltered data. Therefore, one concludes that this procedure is really important because it reflects the influence of the "hidden" external factors that can be removed with the help of filtration procedure.

Results and Discussion

In this paper we show how to create a "universal" platform based on the 3D-DGI – method.

It helps to reduce the large-size initial rectangle matrices and finally one can receive only two parameters (expressed by relationships (1) and (2)) that in many cases are sufficient for solution of the problem formulated in section one. We do believe that these two parameters because of their generality one can find an application in metrology and different nanotechnologies as a simple metrological standard. Besides, it can be used in the industrial electronics when it is necessary to compare the "reference" device (presented mathematically as a rectangle matrix) with the tested one or select the "best" gadget from the existing ones. These two key problems can be solved with the help of expressions (1) and (2). We deliberately imitate this situation with a "similar" experiment that will be frequently met in the industrial applications. The propose method is "universal" and authors are opened for analysis of other interesting data in order to collect necessary statistics associated with this method in order to prove its "universality". It reminds the partition function used in the statistical mechanics when the Hamiltonian operators containing large number of freedom degrees are transformed with the help of partition function to a finite number of thermodynamic parameters. The same procedure is realized with the help of 3D-DGI method. Schematically this reduction can be presented with the help of the following scheme.

$$Hamiltonian(N_1, N_2, N_3 ...) \rightarrow The\ Hibbs\ partition\ funtion \rightarrow (P, V, T, \mu, ...).$$
$$Three\ random\ TLS(s)\ (N_1, N_2, N_3) \rightarrow [3D - DGI - method] \rightarrow (13\ parameters).$$
$$(5)$$

Actually, on can claim that this platform enables to describe a wide set of TLS(s) and transform them to the corresponding 3D-surfaces serving as a specific "fingerprints" of these TLS in the 13-th dimensional features space. Definitely, the authors are going to use this "unexpected finding" and test it on other available data in their further research.

Mathematical Appendix.

In the Mathematical Appendix we describe the mathematical details associated with the derivation of the complete DGI in 3D-space. We remind here that preliminary results based on the application of the incomplete DGI form of the fourth order in 3D space is outlined recently in [8]. Let us consider the power-law form of the fourth order:

$$L_k^{(4)} = A_{40}^{(1,0)}(y_1 - r_{1k})^4 + A_{40}^{(2,0)}(y_2 - r_{2k})^4 + A_{40}^{(3,0)}(y_3 - r_{3k})^4 -$$
$$-B_{22}^{(1,2)}(y_1 - r_{1k})^2 \cdot (y_2 - r_{2k})^2 - B_{22}^{(1,3)}(y_1 - r_{1k})^2 \cdot (y_3 - r_{3k})^2 - B_{22}^{(2,3)}(y_2 - r_{2k})^2 \cdot (y_3 - r_{3k})^2 +$$
$$+C_{211}^{(1,2)}(y_1 - r_{1k})^2 \cdot (y_2 - r_{2k}) \cdot (y_3 - r_{3k}) + C_{211}^{(1,3)}(y_2 - r_{2k})^2 \cdot (y_1 - r_{1k}) \cdot (y_3 - r_{3k}) +$$
$$+C_{211}^{(3,2)}(y_3 - r_{3k})^2 \cdot (y_1 - r_{1k}) \cdot (y_2 - r_{2k}) - \frac{1}{2}D_{31}^{(1,2)}(y_1 - r_{1k}) \cdot (y_2 - r_{2k})\left[(y_1 - r_{1k})^2 + (y_2 - r_{2k})^2\right] -$$
$$-\frac{1}{2}D_{31}^{(1,3)}(y_1 - r_{1k}) \cdot (y_3 - r_{3k})\left[(y_1 - r_{1k})^2 + (y_3 - r_{3k})^2\right] -$$
$$-\frac{1}{2}D_{31}^{(2,3)}(y_2 - r_{2k}) \cdot (y_3 - r_{3k})\left[(y_2 - r_{2k})^2 + (y_3 - r_{3k})^2\right].$$

(A1)

In expression (A1) the upper indices define the combination of the variables y (=1,2,3) fixing the location of an arbitrary point M(y1,y2,y3) in 3D-space, the low indices determine the values of the power-law exponents that correspond to the algebraic form of the fourth order. The choice of the sign's combination ( ) before the constants in (1) will be explained below. Three random sequences are determined by the values r (k =1,2,3; k=1,2,…,N). Expression (1) represents itself the complete form of the fourth order that contains the combination of three variables associated with an

arbitrary point M(y1,y2,y3) and three arbitrary sequences r k. The desired DGI is obtained from the following requirement

$$\frac{1}{N}\sum_{k=1}^{N} L_k^{(4)} = I_4$$

(A2)

In order to remove in expression (A2) the cubic terms we introduce the variables

$$Y_\alpha = y_\alpha - \langle r_\alpha \rangle, \quad \langle r_\alpha \rangle = \frac{1}{N}\sum_{k=1}^{N} r_{\alpha k}$$

(A3)

and nullify the linear terms. This requirement helps us to separate the desired variables Y from each other and keep only the terms of the second and fourth orders, correspondingly. In order to decrease the number of constants in (A2) and derive the DGI not depending on some additional constants one defines three key ratio constants)3,2(,)3,1(,)2,1(=) , (htiw ,) , (R

$$R^{(\alpha,\beta)} = \frac{B^{(\alpha,\beta)}}{A} = \frac{C^{\gamma(\alpha,\beta)}}{A} = \frac{D^{(\alpha,\beta)}}{A},$$
$$A_{40}^{(\alpha)} = A_{40}^{(\beta)} = A_{40}^{(\gamma)} \equiv A, \quad \alpha, \beta, \gamma = 1, 2, 3.$$

(A4)

It is convenient also to introduce the following notations for the integer moments and their intercorrelations and present them as

$$Q_{\alpha^m\beta^n\gamma^l} = \frac{1}{N}\sum_{k=1}^{N}\left((\Delta r_{3k})^m (\Delta r_{2k})^n (\Delta r_{1k})^l\right) \equiv \left\langle (\Delta r_\alpha)^m (\Delta r_\beta)^n (\Delta r_\gamma)^l \right\rangle,$$
$$\alpha \geq \beta \geq \gamma, (\alpha, \beta, \gamma) = 1, 2, 3.$$

(A5)

In the result of the introduced notations (A4) and (A5), the system of linear equations for the finding of unknown ratios R(,) from the nullification requirement of the entering linear terms accepts the form

$$\left[2Q_{221} - Q_{332} + \frac{3}{2}Q_{211} + \frac{1}{2}Q_{222}\right] \cdot R^{(1,2)} +$$
$$+\left[2Q_{331} - Q_{322} + \frac{3}{2}Q_{311} + \frac{1}{2}Q_{333}\right] \cdot R^{(1,3)} - 2Q_{321} \cdot R^{(2,3)} = 4Q_{111},$$
$$\left[2Q_{211} - Q_{331} + \frac{3}{2}Q_{221} + \frac{1}{2}Q_{111}\right] \cdot R^{(1,2)} - 2Q_{321} \cdot R^{(1,3)} +$$
$$+\left[2Q_{332} - Q_{311} + \frac{3}{2}Q_{322} + \frac{1}{2}Q_{333}\right] \cdot R^{(2,3)} = 4Q_{222},$$
$$-2Q_{321} \cdot R^{(1,2)} + \left[2Q_{311} - Q_{221} + \frac{3}{2}Q_{331} + \frac{1}{2}Q_{111}\right] \cdot R^{(1,3)} +$$
$$+\left[2Q_{322} - Q_{211} + \frac{3}{2}Q_{332} + \frac{1}{2}Q_{222}\right] \cdot R^{(2,3)} = 4Q_{333}.$$

(A6a)

The linear system of equations helps to reduce 3 moments (Q333, Q222, Q111) and 7 intercorrelations of the third order (Q332, Q322, Q221, Q211, Q331, Q311, Q321) to calculation of three unknown ratios R(,) only. We should notice also that the combination of the algebraic signs in (1) is chosen in that way for the keeping of the partial solution R=1 of system (A6a) in the case when all three random sequences r k are identical to each other, i.e. r1k = r2k = r3k. It is natural to define it as the case of spherical symmetry. If only two sequences coincide with other (for example, r1k = r2k r3k) then we deal with the case of the cylindrical symmetry. In this case, the linear system (A6a) is reduced to the couple of linear equations relatively the variables R(1,2) R(1,3)=R(2,3). The number of triple correlations equals four in this case (Q111, Q113, Q133, Q333). The system (A6a) is simplified and reduced to the couple of linear equations relatively two variables R(1,2) and R(1,3)

$$\left(4Q_{111} - Q_{333}\right)R^{(1,2)} + \left(2Q_{331} + \frac{1}{2}Q_{333} - \frac{3}{2}Q_{311}\right)R^{(1,3)} = 4Q_{111},$$

$$-2Q_{311}R^{(1,2)} + \left(4Q_{311} - Q_{111} + 3Q_{331}\right)R^{(1,3)} = 4Q_{333}. \tag{A6b}$$

Equations (A6) facilitate considerably the further calculations. After averaging procedure applied to expression (A2) the structure of the fourth order form can be rewritten as

$$K_4\left(Y_1, Y_2, Y_3\right) + K_2\left(Y_1, Y_2, Y_3\right) = I_4 \tag{A7}$$

As before [1-2], we chose the value of the invariant I4 as the double value of the free constant figuring in the left-hand side of (A7). After some algebraic manipulations the fourth and the second order forms entering to the left-hand side can be presented as

$$K_4\left(Y_1, Y_2, Y_3\right) = Y_1^4 + Y_2^4 + Y_3^4 + R^{(1,2)}Y_1Y_2\left[Y_3^2 - \frac{1}{2}\left(Y_1 + Y_2\right)^2\right] +$$
$$+ R^{(1,3)}Y_1Y_3\left[Y_2^2 - \frac{1}{2}\left(Y_1 + Y_3\right)^2\right] + R^{(2,3)}Y_2Y_3\left[Y_1^2 - \frac{1}{2}\left(Y_2 + Y_3\right)^2\right]. \tag{A8a}$$

$$K_2\left(Y_1, Y_2, Y_3\right) = A_{11}Y_1^2 + A_{22}Y_2^2 + A_{33}Y_3^2 +$$
$$+ A_{12}Y_1Y_2 + A_{13}Y_1Y_3 + A_{23}Y_2Y_3. \tag{A8b}$$

The constants Asa denifed era)b8(noisserpxe ni gnirugif

$$A_{11} = 6Q_{11} - \left(Q_{22} + \frac{3}{2}Q_{21}\right)R^{(1,2)} - \left(Q_{33} + \frac{3}{2}Q_{31}\right)R^{(1,3)} + Q_{32}R^{(2,3)},$$

$$A_{22} = 6Q_{22} - \left(Q_{11} + \frac{3}{2}Q_{21}\right)R^{(1,2)} + Q_{31}R^{(1,3)} - \left(Q_{33} + \frac{3}{2}Q_{32}\right)R^{(2,3)},$$

$$A_{33} = 6Q_{33} + Q_{21}R^{(1,2)} - \left(Q_{11} + \frac{3}{2}Q_{31}\right)R^{(1,3)} - \left(Q_{22} + \frac{3}{2}Q_{32}\right)R^{(2,3)},$$

$$A_{12} = -\left(4Q_{21} + \frac{3}{2}Q_{11} + \frac{3}{2}Q_{22} - Q_{33}\right)R^{(1,2)} + 2Q_{32}R^{(1,3)} + 2Q_{31}R^{(2,3)},$$

$$A_{13} = 2Q_{32}R^{(1,2)} - \left(4Q_{31} + \frac{3}{2}Q_{11} + \frac{3}{2}Q_{33} - Q_{22}\right)R^{(1,3)} + 2Q_{12}R^{(2,3)},$$

$$A_{23} = 2Q_{31}R^{(1,2)} + 2Q_{21}R^{(1,3)} - \left(4Q_{32} + \frac{3}{2}Q_{22} + \frac{3}{2}Q_{33} - Q_{11}\right)R^{(2,3)}. \tag{A9}$$

The constant I4 (defined by 3 moments and 12 intercorrelations of the fourth order) figuring in the right-hand side of (A7) is defined as

$$I_4 = Q_{1111} + Q_{2222} + Q_{3333} - \left(Q_{2211} - Q_{3321} + \frac{1}{2}Q_{2111} + \frac{1}{2}Q_{2221}\right)R^{(1,2)} -$$
$$- \left(Q_{3311} - Q_{3221} + \frac{1}{2}Q_{3111} + \frac{1}{2}Q_{3331}\right)R^{(1,3)} -$$
$$- \left(Q_{3322} - Q_{3211} + \frac{1}{2}Q_{3222} + \frac{1}{2}Q_{3332}\right)R^{(2,3)}. \tag{A10}$$

It is interesting to notice that in the case of the spherical symmetry (r1k = r2k = r3k) all correlations coincide with each other and the value of I4 equals zero. The form of the fourth order (A7) admits the separation of the variables in the spherical system of coordinates. If one accepts the conventional notations:

$$y_1 = \langle y_1 \rangle + R\sin\theta\cos\varphi,$$
$$y_2 = \langle y_2 \rangle + R\sin\theta\sin\varphi,$$
$$y_3 = \langle y_3 \rangle + R\cos\theta,$$
$$0 \le \theta \le \pi, 0 \le \varphi \le 2\pi, \tag{A11}$$

then substitution of these variables into (A7) leads to the following biquadratic equation relatively the unknown radius R() ,

$$\left[R(\theta, \varphi)\right]^4 + \left[\frac{P_2(\theta, \varphi)}{P_4(\theta, \varphi)}\right]\left[R(\theta, \varphi)\right]^2 - \frac{I_4}{P_4(\theta, \varphi)} = 0. \tag{A12a}$$

The desired solution (R(θ, φ) > 0) is written as

$$R(\theta, \varphi) = \left[\frac{\sqrt{P_2^2(\theta, \varphi) + 4I_4 \cdot P_4(\theta, \varphi)} - P_2(\theta, \varphi)}{2P_4(\theta, \varphi)}\right]^{\frac{1}{2}} \tag{A12b}$$

The polynomials P2,4(,) entering in (A12) are defined by the following expressions

$$P_4(\theta, \varphi) = \sin^4\theta \cdot \cos^4\varphi + \sin^4\theta \cdot \sin^4\varphi + \cos^4\theta +$$
$$+ R^{(1,2)}\sin^2\theta\sin\varphi\cos\varphi\left[\cos^2\theta - \frac{\sin^2\theta}{2}(\sin\varphi + \cos\varphi)^2\right] +$$
$$+ R^{(1,3)}\sin\theta\cos\theta\cos\varphi\left[\sin^2\theta\sin^2\varphi - \frac{1}{2}(\sin\theta\cos\varphi + \cos\theta)^2\right] +$$
$$+ R^{(2,3)}\sin\theta\cos\theta\sin\varphi\left[\sin^2\theta\cos^2\varphi - \frac{1}{2}(\sin\theta\sin\varphi + \cos\theta)^2\right] \tag{A13a}$$

$$P_2(\theta, \varphi) = A_{11}\sin^2(\theta)\cos^2(\varphi) + A_{22}\sin^2(\theta)\sin^2(\varphi) + A_{33}\cos^2(\theta) +$$
$$+ A_{12}\sin^2(\theta)\sin(\varphi)\cos(\varphi) + A_{13}\sin(\theta)\cos(\theta)\cos(\varphi) + A_{23}\sin(\theta)\cos(\theta)\sin(\varphi). \tag{A13b}$$

The last expressions (A11)-(A13) determine the final form of the DGI in 3D-space. It includes three surfaces determined by expressions (A11). The further analysis shows that expression (12b) equals zero (because I4 = 0) in the case of the coincidence of three compared random sequences (r1k = r2k = r3k). The radius R(,) can contain the complex expression when the integrand in (A12b) becomes negative. It accepts the negative values when the constant I4 in the most cases defined by expression (A10) becomes negative. In this case, it is convenient to rewrite expressions (A11) in the form

$$y_1 = \langle y_1 \rangle + |R(\theta, \varphi)|\sin\theta\cos\varphi,$$
$$y_2 = \langle y_2 \rangle + |R(\theta, \varphi)|\sin\theta\sin\varphi,$$
$$y_3 = \langle y_3 \rangle + |R(\theta, \varphi)|\cos\theta,$$
$$|R(\theta, \varphi)| = \sqrt{\left[\operatorname{Re}(R(\theta, \varphi))\right]^2 + \left[\operatorname{Im}(R(\theta, \varphi))\right]^2},$$
$$0 \le \theta < \pi, 0 \le \varphi < 2\pi. \tag{A14a}$$

Three other "imaginary" surfaces (when I4 < 0) can be necessary for more detailed analysis

$$Y_1 = |\operatorname{Im}(R(\varphi, \theta))|\cos(\varphi)\sin(\theta),$$
$$Y_2 = |\operatorname{Im}(R(\varphi, \theta))|\sin(\varphi)\sin(\theta),$$
$$Y_3 = |\operatorname{Im}(R(\varphi, \theta))|\cos(\theta)$$
$$0 \le \varphi < 2\pi, 0 \le \theta < \pi. \tag{A14b}$$

Finishing this extended Appendix one can conclude that this method (free from treatment errors and model assumptions) represents itself a "universal" platform that can be used from comparison of different data expressed in the form of rectangle matrices. Really, any initial matrix N×M (N is a number of data points, N>M, M is a number of columns) is reduced to the matrix M×Prm (Prm=13) that can be used for the further manipulations. The most significant part is related to the radius modulus) , (R in expression (14a) and, namely, this surface will be used for reduction purposes.

References

1. Timashev, Serge F, and Yuriy S Polyakov. "Review of flicker noise spectroscopy in electrochemistry." Fluctuation and Noise letters 7 (2007): R15-R47.

2. Yulmetyev, Renat, Peter Hanggi, and Fail Gafarov. "Stochastic dynamics of time correlation in complex systems with discrete time." Physical Review E 62 (2000): 6178.

3. Yulmetyev, Renat, Peter Hanggi, and Fail Gafarov. "Quantification of heart rate variability by discrete nonstationary non-Markov stochastic processes." Physical Review E 65 (2002): 046107.

4. Nigmatullin, Raoul R., and Artem S. Vorobev. "The "Universal" Set of Quantitative Parameters for Reading of the Trendless Sequences." Fluctuation and Noise Letters 18 (2019): 1950023.

5. Nigmatullin, Raoul R. "Discrete Geometrical Invariants in 3D Space: How Three Random Sequences Can Be Compared in Terms of "Universal" Statistical Parameters." Frontiers in Physics 8 (2020): 76.